Air-Conditioning, Heating, and Refrigeration Institute (AHRI) Low-GWP Alternative Refrigerants Evaluation Program (Low-GWP AREP)

TEST REPORT #41

System Drop-In Tests of Refrigerant Blend DR-34 (R-452A) in a Trailer Refrigeration Unit Designed for R-404A

Michal Hegar
Michal Kolda

Ingersoll-Rand
Engineering and Technology Center, Prague,
Florianova 2460, Hostivice
Czech Republic

January 13, 2015

This report has been made available to the public as part of the author company's participation in the AHRI's Low-GWP AREP.

Air-Conditioning, Heating, and Refrigeration Institute
2111 Wilson Boulevard, Suite 500
Arlington VA 22201
(703) 524-8800
www.ahrinet.org

Introduction:

This report presents the results of the cooling capacity refrigerant replacement tests on a typical Thermo King trailer refrigeration unit with refrigerant R-404A as a baseline and one alternative blend DR-34 (R-452A) from DuPont.

Cooling capacity tests were performed in the August 2014 in a calorimeter test cell at Ingersoll-Rand's Engineering and Technology Center Prague (ETC Prague), Czech Republic. This calorimeter test cell is an isothermal chamber designed for measuring cooling capacities of truck and trailer units in accordance with AHRI Standard 1110-2013[1].

1. Details of Test Setup:

The unit tested was a Thermo King SLXe-400 trailer refrigeration unit and it employs R-404A as the refrigerant. The unit's rated net cooling capacities was determined at high speed engine operation under the following ATP[2] conditions; 17.4 kW at 30 ºC ambient / 0 ºC evaporator return air temperatures and 9.3 kW at 30 °C ambient / -20 °C evaporator return air temperatures. The unit works with a Thermo King open-shaft 4 cylinder reciprocating compressor with a displacement of 492 cm^3 (30 cu in). The compressor is driven from a diesel engine or from an electric motor in standby mode. The diesel engine and electric motor are both integrated in the unit. All tests were performed with the Thermo King standard 35 cSt polyol ester compressor lubricant.

The tested unit was installed in the test chamber and the lab technology maintained required temperatures inside and outside the chamber. The calorimetric chamber thermal losses are determined before the testing is initialized. During the cooling mode the tested unit dissipates heat generated by electric heaters with fans, which are controlled in order to achieve the requested temperatures. After temperature conditions are stabilized, the cooling capacity is determined from the measured input power to the fans/heaters and thermal losses through chamber walls. The cooling capacity is calculated within a measurement uncertainty of ± 2 % from measured values.

Table 1 summarizes the cooling capacity tests performed on the SLXe-400 operating on high-speed diesel engine mode. Tests were carried out in compliance with requirements defined in AHRI Standard 1110-2013 and cooling capacities are reported under the standard rating conditions. Cooling capacities are also reported under ATP rating conditions for mechanically refrigerated equipment.

[1] ANSI/AHRI Standard 1110 2013 Standard for Performance Rating of Mechanical Transport Refrigeration Units
[2] Agreement on the International Carriage of Perishable Foodstuffs and on the Special Equipment to be Used for Such Carriage (ATP). UNECE Transport Division publication ECE/TRANS/219.

Condenser Air Inlet Temperature (CAIT)		Evaporator Air Inlet Temperature (EAIT)		Note:
[°C]	[°F]	[°C]	[°F]	
37.8	100	1.7	35	AHRI condition
37.8	100	-17.8	0	AHRI condition
37.8	100	-28.9	-20	Added condition
30	86	0	32	ATP condition
30	86	-20	-4	ATP condition

Table 1: Test temperature conditions

The refrigeration system cycle diagram and probe placements are illustrated in Figure 1. All tests were conducted with DR-34 refrigerant placed in the representative unit with no system modifications except thermal expansion valve adjustments.

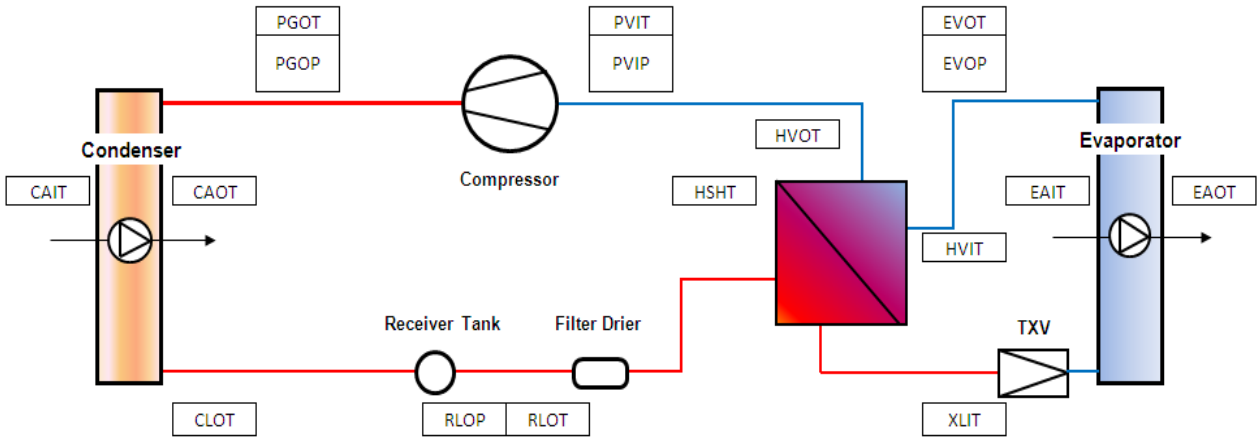

Figure 1: The refrigeration cycle diagram and probe placement

Measurement instrumentation:
Temperature sensors Pt 100, T 1025 and T 1027 class A
Pressure transducers DMP 331 and DMP 333
Electronic scales Soehnle Proffesional
Power input measurement Contes system Domino, type PAWH

The ETC Prague has ISO 9001 certification. All the testing equipment and measuring devices used are regularly inspected and calibrated.

Testing sensors nomenclature:

CAIT	Condenser Air Inlet Temperature
CAOT	Condenser Air Outlet Temperature
CLOT	Condenser Liquid Outlet Temperature
EAIT	Evaporator Air Inlet Temperature
EAOT	Evaporator Air Outlet Temperature
EVOP	Evaporator Vapor Outlet Pressure
EVOT	Evaporator Vapor Outlet Temperature
ESHT	Evaporator Superheat Temperature
HSHT	Heat Exchanger Superheat Temperature
HVIT	Heat Exchanger Vapor Inlet Temperature
HVOT	Heat Exchanger Vapor Outlet Temperature
PGOP	Compressor Gas Outlet Pressure
PGOT	Compressor Gas Outlet Temperature
PSHT	Compressor Superheat Temperature
PVIP	Compressor Vapor Inlet Pressure
PVIT	Compressor Vapor Inlet Temperature
RLOP	Receiver Liquid Outlet Pressure
XLIT	Expansion Valve Liquid Inlet Temperature

The tested unit was charged with R-404A according to the unit specification and the thermal expansion valve (TXV) setting was verified. After the nominal cooling capacity was verified at ATP standard rating conditions (-20 °C temperature inside the chamber and 30 °C ambient temperature) on high-speed diesel engine mode and on electric stand-by mode, cooling capacity tests were performed at high diesel engine speed mode and at electric standby mode under the temperature conditions shown in Table 1. Diesel fuel consumption was measured for all tested conditions at diesel engine mode and electric energy consumption was measured for all tested conditions at electric stand-by mode.

After the baseline tests were completed, the R-404A refrigerant was recovered, the filter drier and oil replaced with the same as the original filter drier and oil, and the unit was then charged with DR-34 refrigerant. The same charge of DR-34 as original R-404A was determined as an optimal amount at initial phase of testing. TXV position was adjusted at ATP standard rating conditions (-20 °C temperature inside the chamber and 30 °C ambient temperature) on high-speed diesel engine mode in order to achieve maximal cooling capacity at these conditions.

2. Results

The following table and charts present a comparison summary of the results calculated from measurements. The TXV was adjusted with focus on maximal cooling capacity at standard ATP rating conditions. The refrigerant properties were provided by DuPont for DR-34, REFPROP version 8 was used for properties of R-404A. The evaporator superheat temperature, ESH, is calculated as a difference between the temperature measured at the evaporator outlet, EVOT, and evaporating temperature, $EVOT_{sat}$. The evaporating temperature, $EVOT_{sat}$, is a function of the evaporating pressure, EVOP, and therefore the NIST database REFPROP version 8 was used for the correct determination of evaporating and condensing temperatures.

The net cooling capacity was determined from measured input power of fans/heaters and thermal losses through the chamber walls. Coefficient of performance (COP) was determined from the measurement at stand-by mode, fuel efficiency ratio (FER) was determined from the measurement at diesel engine high speed mode.

The following calculations were employed for determination of differences and ratios relative to R-404A and DR-34 refrigerant. Table 2 shows the comparison of DR-34 main parameters relative to the R-404A baseline.

Evaporator temp. difference: $d(EVOT_{sat}) = (EVOT_{sat})_{DR-34} - (EVOT_{sat})_{R-404A}$ [°F]

Evaporator superheat difference: $d(ESH) = ESH_{Alt} - ESH_{R-404A}$ [°F]

Condensing temp. difference: $d(PGOT_{sat}) = (PGOT_{sat})_{DR-34} - (PGOT_{sat})_{R-404A}$ [°F]

Suction pressures difference: $d(PVIP) = PVIP_{DR-34} - PVIP_{R-404A}$ [psia]

Suction temperatures difference: $d(PVIT) = PVIT_{DR-34} - PVIT_{R-404A}$ [°F]

Discharge pressures difference: $d(PGOP) = PGOP_{DR-34} - PGOP_{R-404A}$ [psia]

Discharge temperatures difference: $d(PGOT) = PGOT_{DR-34} - PGOT_{R-404A}$ [°F]

Power input ratio: $(P_c)_R = (P_c)_{DR-34}/(P_c)_{R-404A}$ [-]

Diesel consumption ratio: $(C_d)_R = (C_d)_{DR-34}/(C_d)_{R-404A}$ [-]

Net cooling capacity ratio: $(Q_o)_R = (Q_o)_{DR-34}/(Q_o)_{R-404A}$ [-]

Coefficient of performance (COP): $\left(\frac{Q_o}{P_c}\right)_R = \left(\frac{Q_o}{P_c}\right)_{DR-34} \Big/ \left(\frac{Q_o}{P_c}\right)_{R-404A}$ [-]

Fuel efficiency ratio (FER): $\left(\frac{Q_o}{C_d}\right)_R = \left(\frac{Q_o}{C_d}\right)_{DR-34} \Big/ \left(\frac{Q_o}{C_d}\right)_{R-404A}$ [-]

Comparison of DR-34 relative to R-404A														
Conditions			Evaporator		Condenser	Compressor				Unit Parameters			Analysis	
CAIT	EAIT	Engine speed	d(EVOT_sat)	d(ESH)	d(PGOT_sat)	d(PVIP)	d(PVIT)	d(PGOP)	d(PGOT)	Pc_R	Cd_R	Qo_R	COP_R	FER_R
[°F]	[°F]	[-]	[°F]	[°F]	[°F]	[psia]	[°F]	[psia]	[°F]	[-]	[-]	[-]	[-]	[-]
86	-4	Stand-by	4.3	-2.4	4.7	-0.9	-2.7	8.1	5.9	-1.2%		-1.7%	-0.4%	
86	-4	HS	5.6	-3.5	5.9	-0.1	-3.1	13.5	6.3		-0.5%	-1.3%		-0.9%
86	32	Stand-by	4.7	-5.8	4.9	-0.2	-3.8	12.0	4.3	0.3%		0.1%	-0.2%	
86	32	HS	5.9	-3.9	6.6	0.7	-0.4	18.4	4.7		0.4%	-0.2%		-0.6%
100	-20	Stand-by	5.0	-5.3	3.9	-0.7	-2.7	6.4	5.6	-1.6%		-4.9%	-3.3%	
100	-20	HS	4.8	-3.1	5.0	-0.8	-2.5	11.5	5.9		-0.9%	-5.5%		-4.7%
100	0	Stand-by	2.4	-3.4	3.8	-1.3	-0.9	6.6	4.1	-1.3%		-2.1%	-0.8%	
100	0	HS	2.7	-2.5	4.0	-1.1	-0.9	8.3	4.5		-0.5%	-3.2%		-2.7%
100	35	Stand-by	4.4	-2.3	4.4	-0.8	-1.8	11.6	2.3	0.0%		0.3%	0.3%	
100	35	HS	2.9	-2.4	5.5	-1.1	-0.4	18.5	2.5		-0.3%	-0.9%		-0.6%

Table 2: Comparison of main parameters for system charged DR-34 relative to R-404A

Overall test results are illustrated in Figures 2 to 11.

3. Evaluation

Figure 2 and 3 show comparison of net cooling capacity for DR-34 relative to R-404A. The cooling capacity at ambient temperature 100 °F was down 5.5 % for DR-34 at low return air temperature (-20 °F) and at compressor high speed. At higher return air temperatures (35 °F) the cooling capacity was practically comparable to R-404A. The cooling capacity at ambient temperature 86 °F has the same trend, the absolute difference of capacity between R-404A and DR-34 is smaller in this case.

Comparison of compressor discharge pressure relative to R-404A is shown in Figures 4 and 5. The measured discharge pressure for the unit charged with DR-34 was higher up to 18.8 psia at high return air temperature compared to R-404A. At low return air temperature the discharge pressure for DR-34 was higher up to 6.4 psia compared to R-404A.

Comparison of compressor discharge temperature relative to R-404A is shown in Figures 6 and 7. The measured compressor discharge temperature was higher up to 6 °F for the circuit working with DR-34 at low return air temperature.

Comparison of coefficient of performance (COP) relative to R-404A is shown in Figures 8 and 9. COP was determined from measurement at stand-by mode as ratio of net cooling capacity and unit input power. The coefficient of performance was lower up to 3.3 % for the circuit working with DR-34 at low return air temperature.

Comparison of fuel efficiency ratio (FER) relative to R-404A is shown in Figures 10 and 11. FER was determined from measurement at diesel HS mode as ratio of net cooling capacity and one hour fuel consumption. The fuel efficiency ratio was lower up to 4.7 % for the circuit working with DR-34 at low return air temperature.

Take notice of insignificant differential values between R-404A and DR-34. The differences are very often lower than a measurement uncertainty. The trends are consistent in both of the conditions (AHRI, ATP).

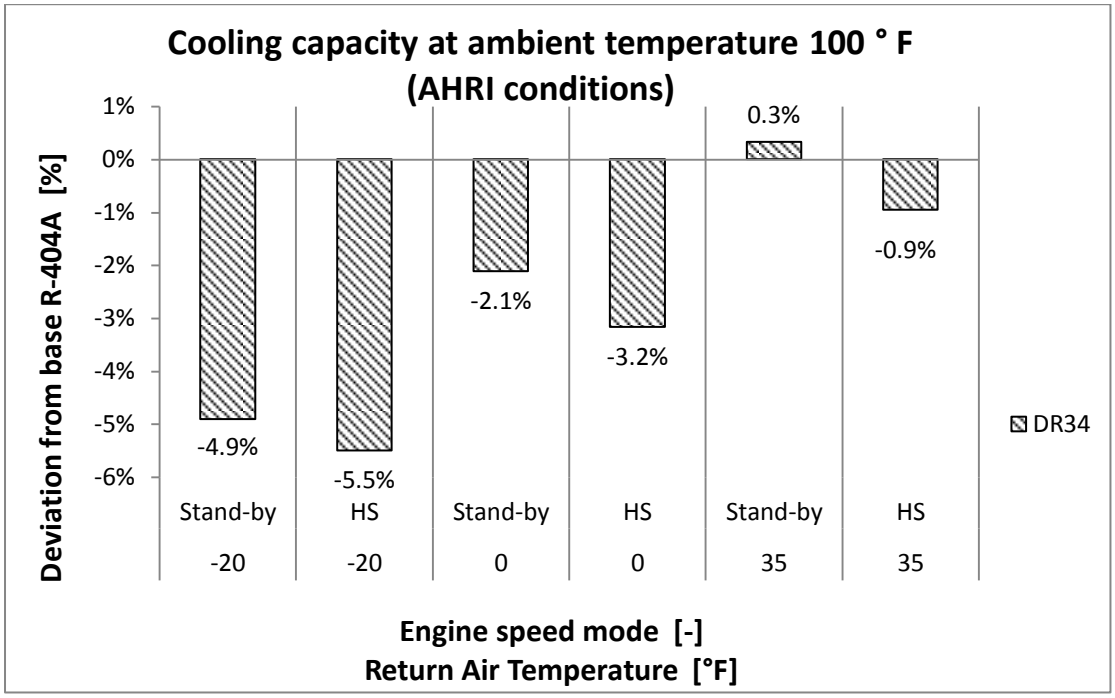

Figure 2: Comparison of net cooling capacity relative to R-404A under AHRI conditions.

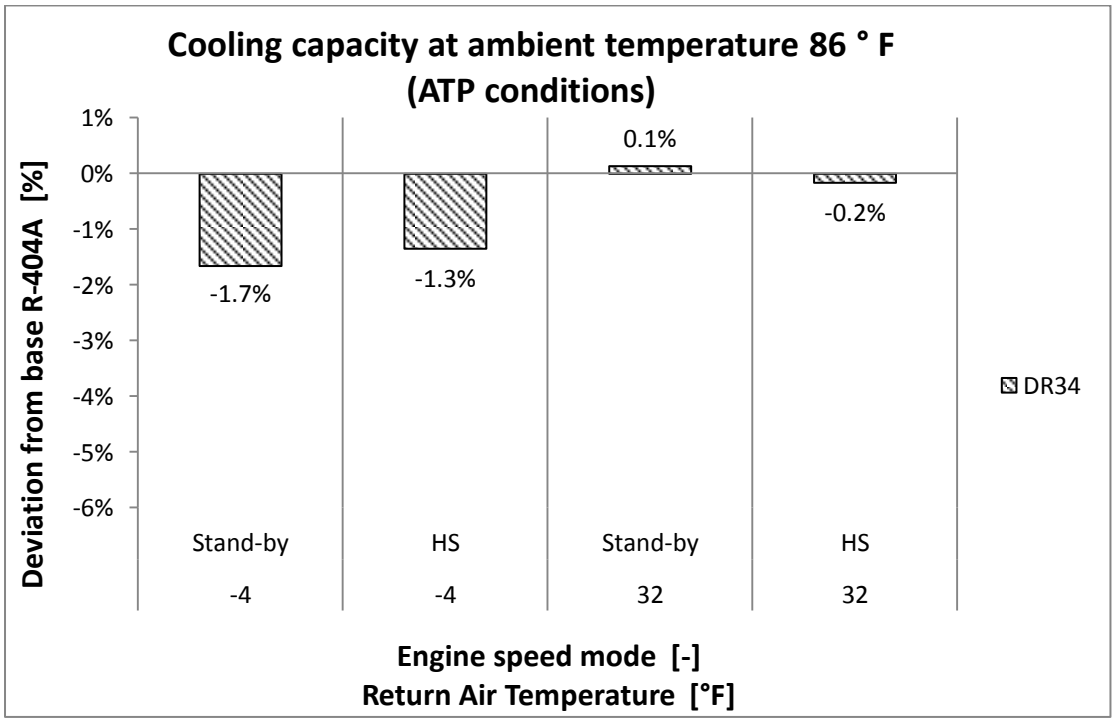

Figure 3: Comparison of net cooling capacity relative to R-404A under ATP conditions.

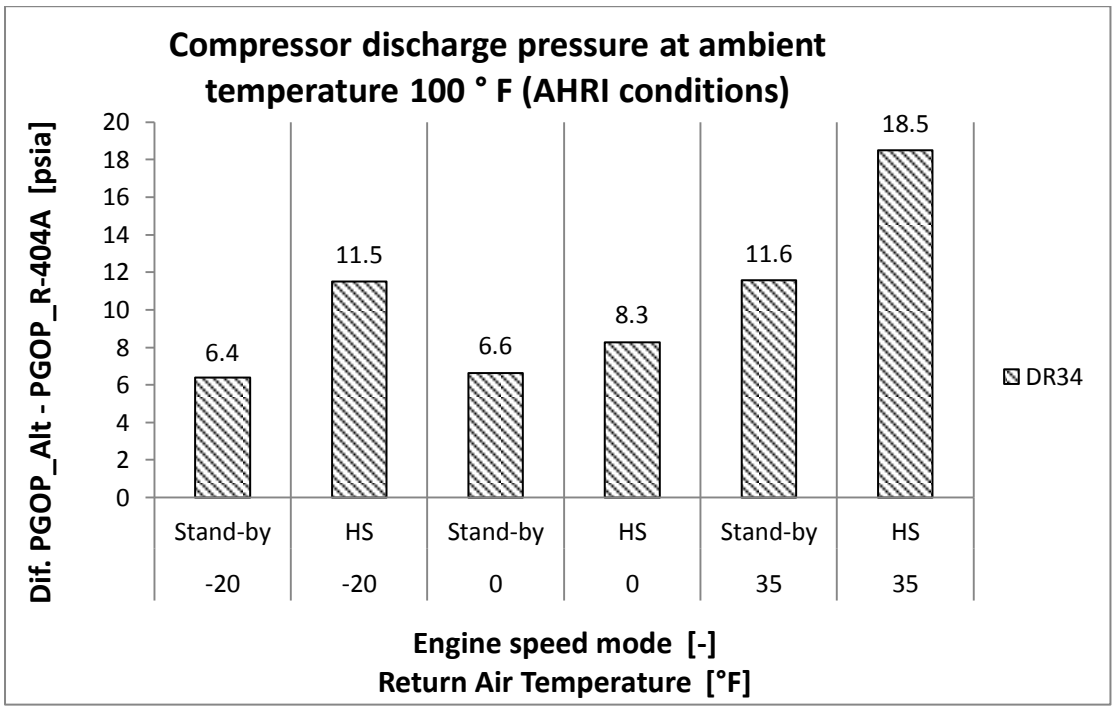

Figure 4: Comparison of compressor discharge pressure relative to R-404A under AHRI conditions.

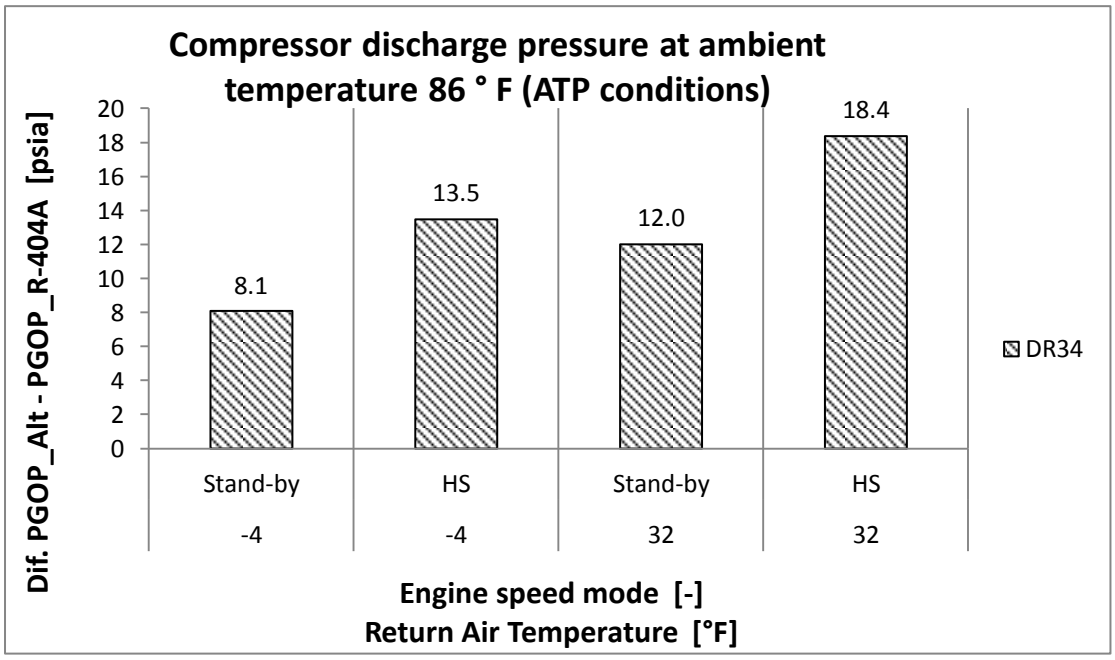

Figure 5: Comparison of compressor discharge pressure relative to R-404A under ATP conditions.

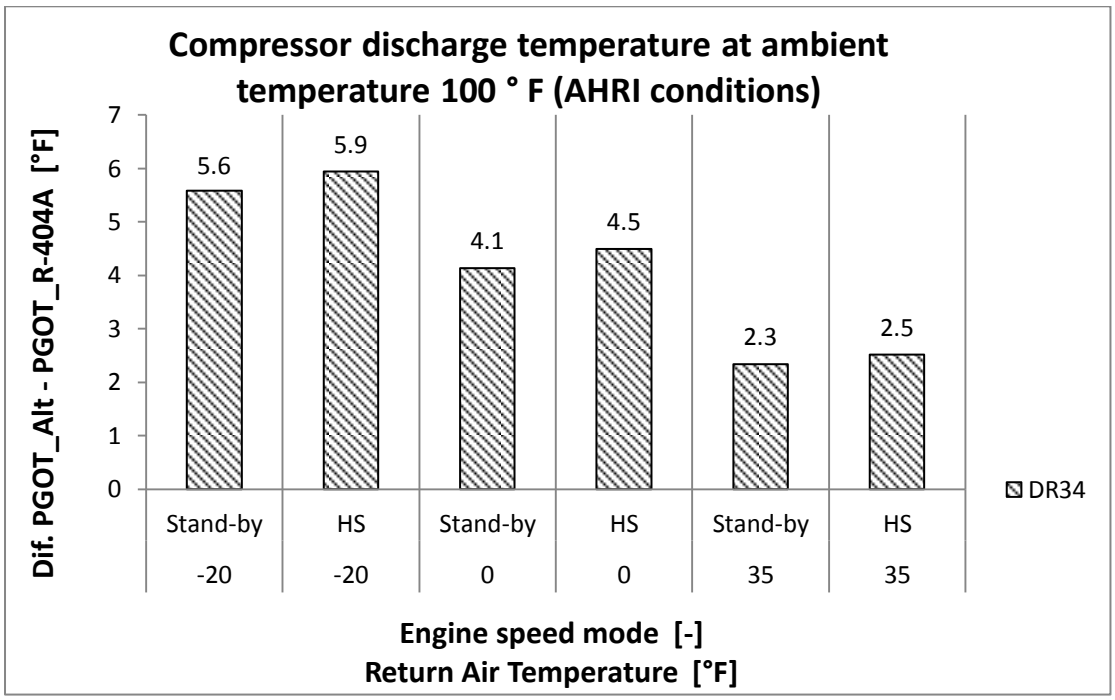

Figure 6: Comparison of compressor discharge temperature relative to R-404A under AHRI conditions.

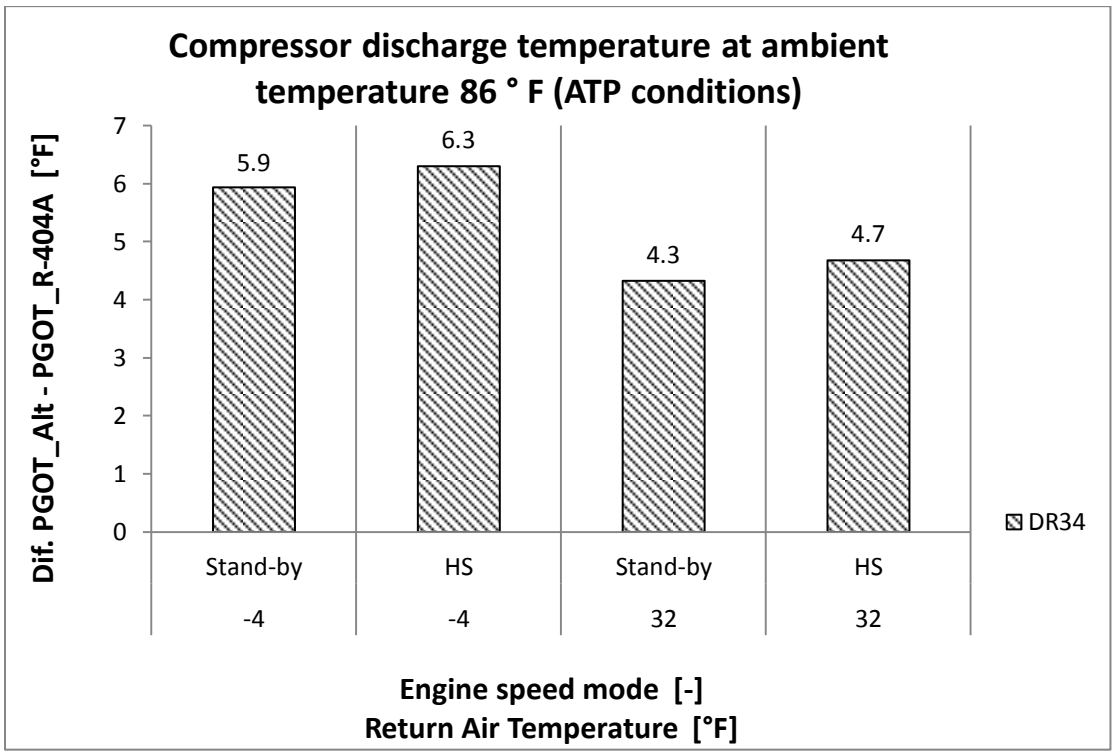

Figure 7: Comparison of compressor discharge temperature relative to R-404A under ATP conditions.

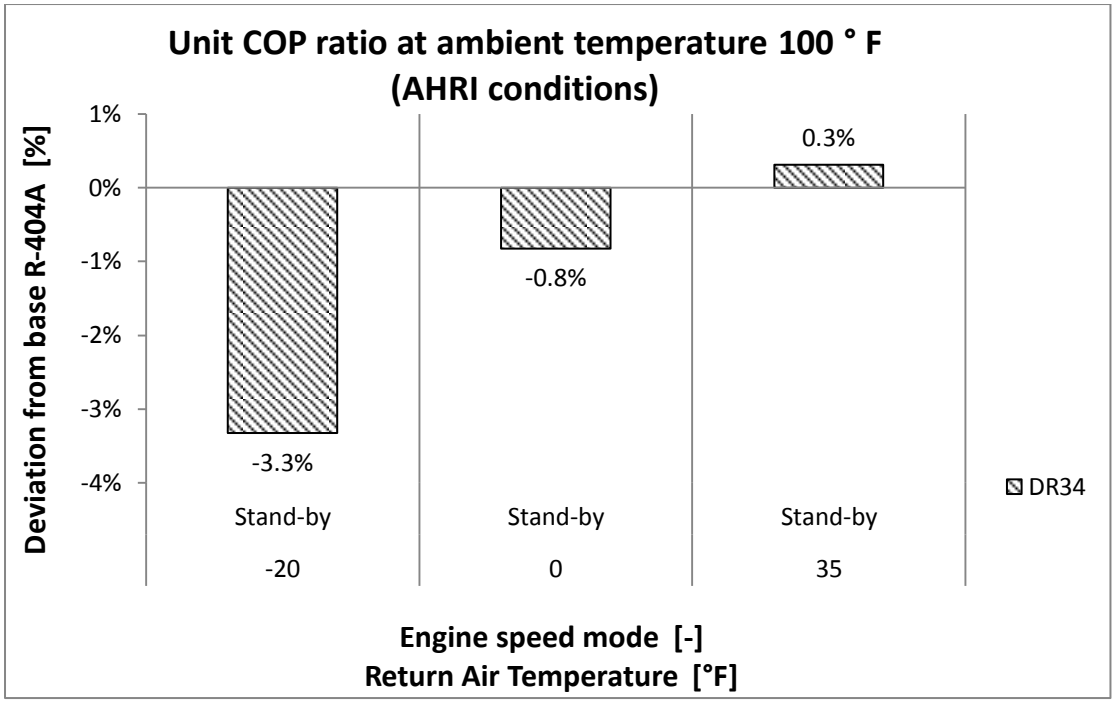

Figure 8: Comparison of COP relative to R-404A under AHRI conditions.

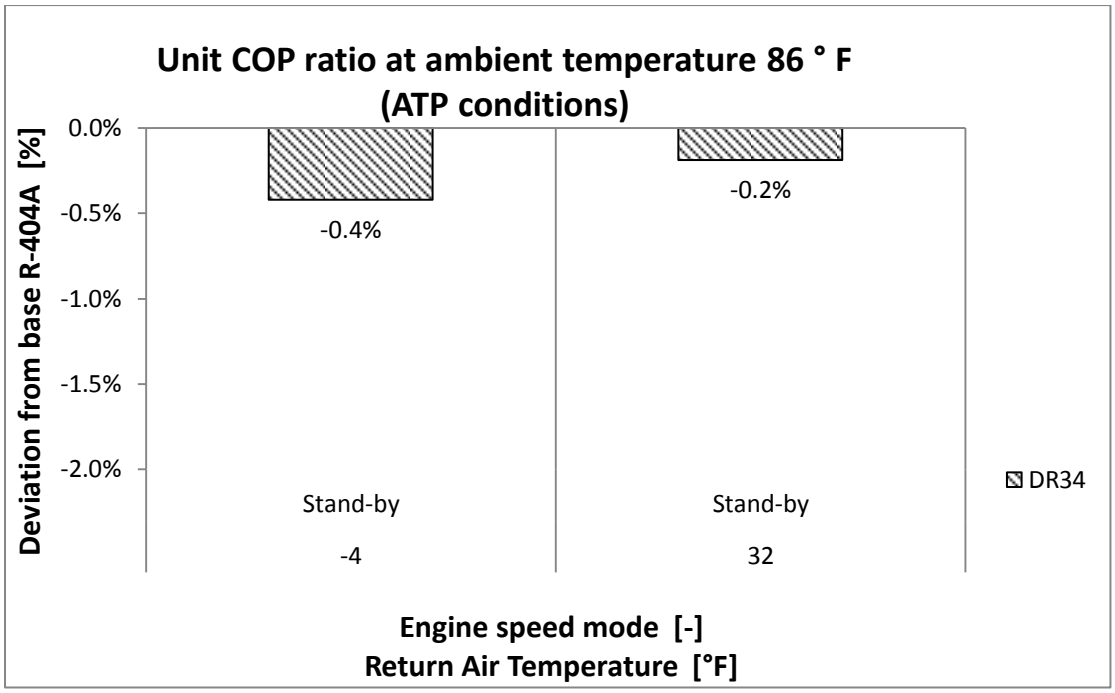

Figure 9: Comparison of COP relative to R-404A under ATP conditions

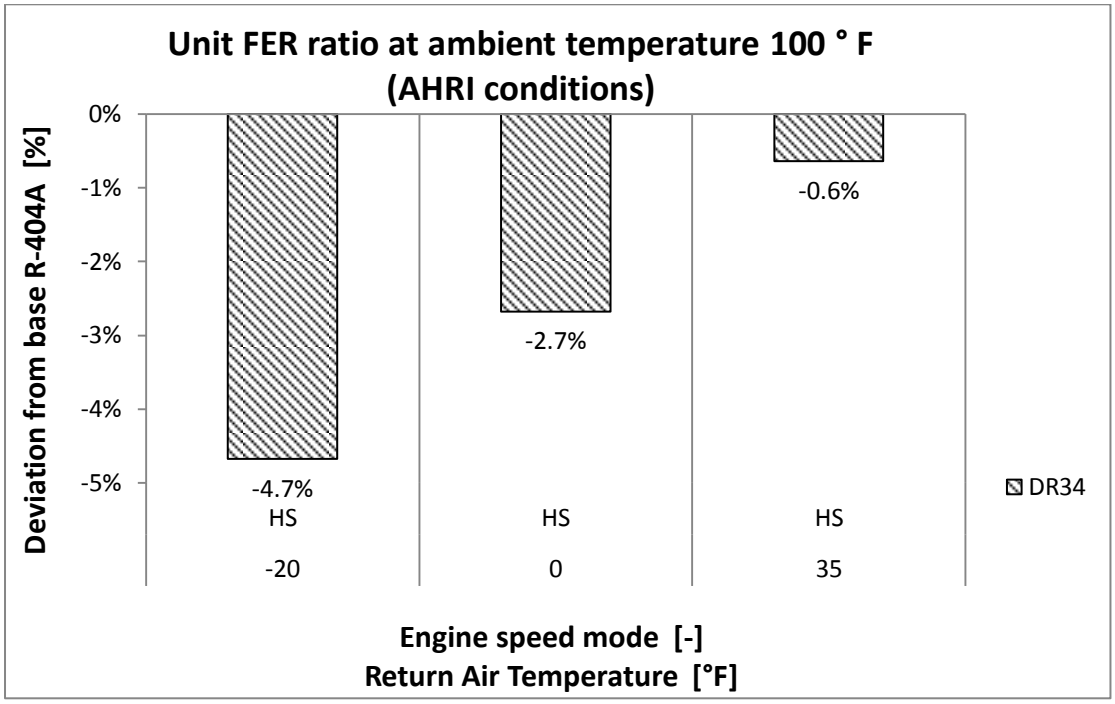

Figure 10: Comparison of FER relative to R-404A under AHRI conditions.

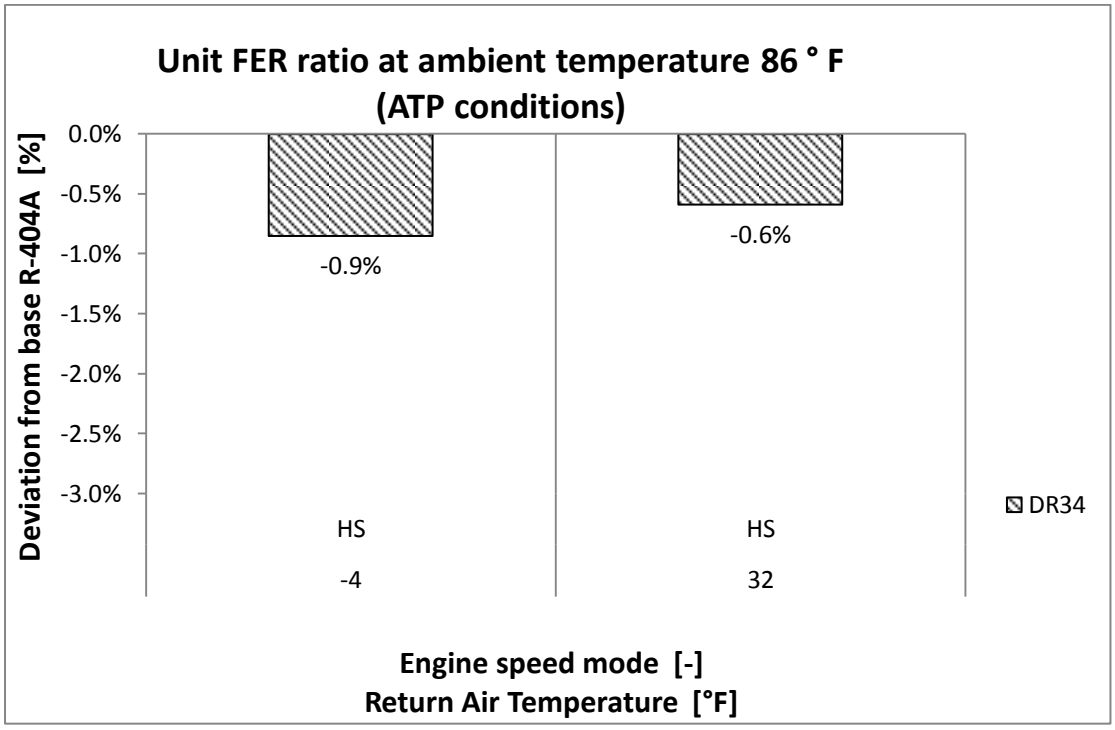

Figure 11: Comparison of FER relative to R-404A under ATP conditions.